Semileptonic $B_s \to K_0^*(1430)$ transitions with the light-cone sum rules

R. Khosravi*
Department of Physics, Isfahan University of Technology, Isfahan 84156-83111, Iran
Department of Physics, Shiraz University, Shiraz 71454, Iran

In the $SU(3)_F$ symmetry limit, using two- and three-particle distribution amplitudes of $B^{\pm}$-meson for B_s, the transition form factors of semileptonic $B_s \to K_0^*(1430)$ decays are calculated in the framework of the light-cone sum rules. The two-particle distribution amplitudes, $\varphi_+(\omega)$ and $\varphi_-(\omega)$ have the most important contribution in estimation of the form factors $f_+(q^2)$, $f_-(q^2)$ and $f_T(q^2)$. The knowledge of the behavior of $\varphi_+(\omega)$ is still rather limited. Therefore, we consider three different parametrizations for the shapes of $\varphi_+(\omega)$ that are derived from the phenomenological models. Using the form factors f_+, f_- and f_T, the semileptonic $B_s \to K_0^*(1430) l\bar{\nu}_l$ and $B_s \to K_0^*(1430) l\bar{l}/\nu\bar{\nu}$, $l = e, \mu, \tau$ decays are analyzed. The branching fractions for the aforementioned decays, in addition the longitudinal lepton polarization asymmetries are calculated. A comparison between our results with predictions of other approaches is provided.

arXiv:2203.09997v1 [hep-ph] 18 Mar 2022

I. INTRODUCTION

The scalar meson is a meson with total spin 0 and even parity. They are often produced in proton-antiproton annihilation, decays of heavy flavor mesons, meson-meson scattering, and radiative decays of vector mesons. Among the scalar mesons, study of the light scalar mesons up to 1.5 GeV is important because their quark content is still a common problem for high energy physics and may be explained in a number of different ways, for example, considering as a meson-meson molecules state [1] or as a tetraquark multiplet [2].

According to the quark model, the scalar mesons about 1 GeV are arranged into two $SU(3)$ nonets, in two scenarios:

Scenario 1 (S1): the light scalar mesons are assumed to compose from two quarks. The nonet mesons below 1 GeV are treated as the lowest lying states, and the nonet mesons near 1.5 GeV are the excited states corresponding to the lowest lying states.

Scenario 2 (S2): the nonet mesons below 1 GeV may be considered as four-quark bound states, and the other nonet mesons are composed from two quarks and viewed as the lowest lying states.

Both scenarios in quark model agree that $K_0^*(1430)$ with the mass of greater than 1 GeV is a scalar meson with two quarks dominated by the $s\bar{u}$ or $s\bar{d}$ state. However in S1, it is regarded as an excited state, and in S2, it is seen as a ground state. In the framework of the light-cone sum rules (LCSR), differences between $K_0^*(1430)$ states in the two scenarios are applied through different distribution amplitudes (DA's) and decay constants [3].

In this paper, our aim is to consider the semileptonic transitions of B_s to $K_0^*(1430)$ in the LCSR using the B_s-meson DA's. In usual, the LCSR method is applied to calculate the form factors of the heavy-to-light decays by utilizing the light meson DA's. For this purpose, two-point correlation function is written based on the light meson. Therefore, light-cone distribution amplitudes (LCDA's) of the light meson appear in theoretical calculations of the correlation function [4–12]. The LCDA's of the light mesons are related to the dynamics of partons in long distance. Still, there is very limited knowledge of the nonperturbative parameters determining these LCDA's. In the case of the light scalar mesons, including $K_0^*(1430)$, this problem is twofold because their internal structures are basically unknown. For this reason, it is necessary to use a method of calculation that is independent of the DA's of the scalar mesons.

In a new approach to the LCSR method related to the semileptonic B decays, it was proposed to insert the correlation function between vacuum and B-meson [13]. In this technique the so-called soft or endpoint, the correlation function is expanded in terms of the DA's of B-meson, near the light-cone region [14, 15]. Therefore, the transition form factors for exclusive decays of B to light mesons are connected to the DA's that depend on the dynamical information of B-meson. Two-particle DA of B-meson, $\varphi_+(\omega)$ plays a particularly prominent role in this new approach to exclusive semileptonic decays. The knowledge of the behavior of $\varphi_+(\omega)$ is still rather limited due to the poor understanding of nonperturbative QCD dynamics (for instance, see Refs. [16–19]). So far, several models for the shape of $\varphi_+(\omega)$ have been proposed based on the QCD sum rules (QCDSR) [20, 21], the LCSR [22–28], and the QCD factorization [29]. Also, the functional form of the three-particle B-meson DA's have been estimated in several models [14, 29, 30].

In this work, the form factors of the semileptonic $B_s \to K_0^*(1430)$ transitions are investigated in the new approach of the LCSR with the two- and three-particle DA's of B_s-meson in the $SU(3)_F$ symmetry limit. Utilizing these form factors, the semileptonic $B_s \to K_0^*(1430) l\bar{\nu}_l$ and $B_s \to K_0^*(1430) l\bar{l}/\nu\bar{\nu}$, $l = e, \mu, \tau$ decays are analyzed. In the

* e-mail: rezakhosravi @iut.ac.ir

standard model (SM), the rare semileptonic $B_s \to K_0^*(1430)l\bar{l}$ decays occur at loop level instead of tree level, by electroweak penguin and weak box diagrams via the flavor changing neutral current (FCNC) transitions of $b \to dl^+l^-$ at quark level. In particle physics, reliable considering of the FCNC decays of B-meson is very important since they are sensitive to new physics (NP) contributions to penguin operators. So, to test the SM and look for NP, we need to determine the SM predictions for FCNC decays and compare these results to the corresponding experimental values.

This work is organized as follows: In Sec II, according to the effective weak Hamiltonian of the FCNC transition $b \to d\ l^+l^-$, the form factors of the semileptonic $B_s \to K_0^*$ decays are calculated with the LCSR model using the B_s-meson DA's. These form factors are basic parameters in studying the forward-backward asymmetry, longitudinal lepton polarization asymmetry and branching fraction of semileptonic decays. Our numerical and analytical results and their comparison with the predictions of other approaches are presented in Sec III. The last section is dedicated to conclusion. Future experimental measurement can give valuable information about these aforesaid decays and the nature of the scalar meson $K_0^*(1430)$.

II. $B_s \to K_0^*\, l^+l^-$ FORM FACTORS WITH THE LCSR

According to the effective weak Hamiltonian of the $b \to d\ l^+l^-$ transition presented in Appendix, the matrix element for the FCNC decay $b \to d$ can be written as:

$$\mathcal{M} = \frac{G_F\alpha}{2\sqrt{2}\pi}V_{tb}V_{td}^*\left[C_9^{\text{eff}}\ \bar{d}\gamma_\mu(1-\gamma_5)b\ \bar{l}\gamma_\mu l + C_{10}\ \bar{d}\gamma_\mu(1-\gamma_5)b\ \bar{l}\gamma_\mu\gamma_5 l - 2\,C_7^{\text{eff}}\ \frac{m_b}{q^2}\,\bar{d}\ i\sigma_{\mu\nu}q^\nu(1+\gamma_5)b\ \bar{l}\gamma_\mu l\right], \tag{1}$$

where G_F is the Fermi constant, α is the fine structure constant at Z mass scale, and V_{ij} are elements of the Cabbibo-Kobayashi-Maskawa (CKM) matrix. $\bar{d}\gamma_\mu(1-\gamma_5)b$ and $\bar{d}\sigma_{\mu\nu}q^\nu(1+\gamma_5)b$ are the transition currents denoted with J_μ^{V-A} and J_μ^T, respectively. This decay amplitude also contains two effective Wilson coefficients C_7^{eff} and C_9^{eff}, where $C_7^{\text{eff}} = C_7 - C_5/3 - C_6$ and C_9^{eff} is explained in Appendix.

To investigate the form factors of $B_s \to K_0^* l^+l^-$ decays via the LCSR, the two-point correlation functions are constructed from the transition currents $J_\mu^{V-A(T)}$, and interpolating current $J^{K_0^*}$ of the scalar meson K_0^*, inserted between vacuum and B_s-meson as follows:

$$\Pi_\mu^{V-A(T)}(p',q) = i\int d^4x\ e^{ip'.x}\langle 0|T\left\{J^{K_0^*}(x)J_\mu^{V-A(T)}(0)\right\}|B_s(p)\rangle, \tag{2}$$

where T is the time ordering operator, $J^{K_0^*} = \bar{s}(x)d(x)$ and $q = p - p'$. The external momenta p' and q are related to the interpolating and transition currents, $J^{K_0^*}$ and $J_\mu^{V-A(T)}$ respectively, so that $p^2 = (p'+q)^2 = m_B^2$. The leading-order diagram for $B_s \to K_0^* l^+l^-$ decays is depicted in Fig. 1.

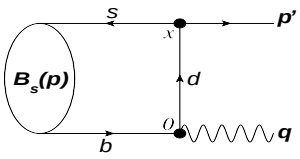


FIG. 1: leading-order diagram for $B_s \to K_0^* l^+l^-$ decays.

The correlation functions in Eq. (2) are complex quantities and have two aspects: phenomenological and theoretical. Hadronic parameters like form factors appear in the phenomenological or physical representation of the correlation functions. The theoretical or QCD side of the correlation functions is obtained in terms of the DA's of B_s-meson. Equating coefficients of the corresponding lorentz structures from both representations through the dispersion relation,

$$\Pi_\mu(p',q) = \frac{1}{\pi}\int_0^\infty ds\frac{\text{Im}\,\Pi_\mu(s)}{s-p'^2}\,, \tag{3}$$

and applying Borel transformation to suppress the contributions of the higher states and continuum, the form factors are calculated from the LCSR.

Inserting a complete set of intermediate states with the same quantum number as the interpolating current $J^{K_0^*}$, in Eq. (2), and isolating the pole term of the lowest scalar meson K_0^*, and then applying Fourier transformation, the

phenomenological representations of the correlation functions are obtained, as follows:

$$\Pi_\mu^{V-A(T)}(p',q) = \frac{1}{m_{K_0^*}^2-p'^2}\langle 0|J^{K_0^*}(p')|K_0^*(p')\rangle\langle K_0^*(p')|J_\mu^{V-A(T)}|B_s(p)\rangle + \sum_h \frac{1}{m_h^2-p'^2}\langle 0|J^{K_0^*}(p')|h(p')\rangle\langle h(p')|J_\mu^{V-A(T)}|B_s(p)\rangle\,. \quad (4)$$

To continue, we define the spectral density functions of higher resonances and the continuum of states as

$$\rho_\mu^{h,V-A(T)}(s) \equiv \pi \sum_h \langle 0|J^{K_0^*}(p')|h(p')\rangle\langle h(p')|J_\mu^{V-A(T)}|B_s(p)\rangle\,\delta(s-m_h^2). \quad (5)$$

Inserting the spectral density functions in Eq. (4), the correlation functions are obtained as

$$\Pi_\mu^{V-A(T)}(p',q) = \frac{1}{m_{K_0^*}^2-p'^2}\langle 0|J^{K_0^*}(p')|K_0^*(p')\rangle\langle K_0^*(p')|J_\mu^{V-A(T)}|B_s(p)\rangle + \frac{1}{\pi}\int_{s_0}^{\infty} ds\frac{\rho_\mu^{h,V-A(T)}(s)}{s-p'^2}, \quad (6)$$

where s_0 is the continuum threshold of K_0^* meson. The matrix element, $\langle 0|J^{K_0^*}|K_0^*\rangle = f_{K_0^*}m_{K_0^*}$, where $f_{K_0^*}$ is the leptonic decay constant of the scalar meson K_0^*. Considering parity and using Lorentz invariance, the transition matrix elements, $\langle K_0^*(p')|J_\mu^{V-A(T)}|B_s(p)\rangle$, can be parametrized as:

$$\begin{aligned}\langle K_0^*(p')|J_\mu^{V-A}|B_s(p)\rangle &= i\left[P_\mu f_+(q^2) + q_\mu f_-(q^2)\right],\\ \langle K_0^*(p')|J_\mu^{T}|B_s(p)\rangle &= -\frac{1}{m_{B_s}+m_{K_0^*}}\left[P_\mu q^2 - q_\mu(m_{B_s}^2-m_{K_0^*}^2)\right] f_T(q^2),\end{aligned} \quad (7)$$

where $f_+(q^2)$, $f_-(q^2)$ and $f_T(q^2)$ are the transition form factors, which only depend on the momentum transfer squared q^2, $P_\mu = (p'+p)_\mu$, and $q_\mu = (p-p')_\mu$. Substituting Eq. (7) in Eq. (6), we obtain

$$\begin{aligned}\Pi_\mu^{V-A}(p',q) &= i f_{K_0^*}m_{K_0^*}\left[\frac{P_\mu f_+(q^2) + q_\mu f_-(q^2)}{m_{K_0^*}^2-p'^2}\right] + \frac{1}{\pi}\int_{s_0}^{\infty} ds\frac{\rho_\mu^{h,V-A}(s)}{s-p'^2},\\ \Pi_\mu^{T}(p',q) &= -\frac{f_{K_0^*}m_{K_0^*}}{m_{B_s}+m_{K_0^*}}\left[\frac{P_\mu q^2 - q_\mu(m_{B_s}^2-m_{K_0^*}^2)}{m_{K_0^*}^2-p'^2}\right] f_T(q^2) + \frac{1}{\pi}\int_{s_0}^{\infty} ds\frac{\rho_\mu^{h,T}(s)}{s-p'^2}\,.\end{aligned} \quad (8)$$

To extract the theoretical or QCD side, the correlation functions in Eq. (2) are expanded in the limit of large m_b in heavy quark effective theory (HQET). In the HQET, the relation between the momentum and four-velocity of B_s-meson is as: $p = m_b v + k$, where k is the residual momentum. Using the relation $p = q + p'$ and $p = m_b v + k$, the four-momentum transfer $\widetilde{q}$ is defined as: $k - p' = q - m_b v \equiv \widetilde{q}$, where $\widetilde{q}$ is called static part of q. Up to $1/m_b$ corrections, the B_s-meson state can be estimated by the relativistic normalization of it $|B_s(p)\rangle = |B_s(v)\rangle$, and the correlation functions $\Pi_\mu^{V-A(T)}(p',q)$ can be approximated to $\widetilde{\Pi}_\mu^{V-A(T)}(p',\widetilde{q})$,

$$\Pi_\mu^{V-A(T)}(p',q) = \widetilde{\Pi}_\mu^{V-A(T)}(p',\widetilde{q}) + \mathcal{O}(1/m_b). \quad (9)$$

Also, the b-quark field is substituted by the effective field as $b(x) = e^{-im_b vx}h_v(x)$. Therefore, the correlation functions in the heavy quark limit, $(m_b \to \infty)$, become [14]:

$$\begin{aligned}\widetilde{\Pi}_\mu^{V-A}(p',\widetilde{q}) &= i\int d^4x\; e^{ip'.x}\langle 0|T\{\bar{s}(x)S_d(x)\gamma_\mu(1-\gamma_5)h_v(0)\}|B_s(v)\rangle,\\ \widetilde{\Pi}_\mu^{T}(p',\widetilde{q}) &= i\int d^4x\; e^{ip'.x}\langle 0|T\{\bar{s}(x)S_d(x)\sigma_{\mu\nu}q^\nu(1+\gamma_5)h_v(0)\}|B_s(v)\rangle.\end{aligned} \quad (10)$$

The full-quark propagator, $S_d(x)$ of a massless quark in the external gluon field in the Fock-Schwinger gauge is as follows [31]:

$$S_d(x) = i\int \frac{d^4k}{(2\pi)^4}e^{-ik.x}\left\{\frac{\not k}{k^2} + \int_0^1 du\; G_{\lambda\rho}(ux)\left[\frac{1}{k^2}ux^\lambda\gamma^\rho - \frac{1}{2k^4}\not k\sigma^{\lambda\rho}\right]\right\}. \quad (11)$$

When the full-quark propagator $S_d(x)$ in Eq. (11) is replaced in Eq. (10), operators between vacuum mode and $B_s(v)$-state create the nonzero matrix elements as $\langle 0|\bar{s}_\alpha(x)h_{v\beta}(0)|B_s(v)\rangle$ and $\langle 0|\bar{s}_\alpha(x)G_{\lambda\rho}(ux)h_{v\beta}(0)|B_s(v)\rangle$. These matrix elements are obtained in terms of two- and three-particle DA's of B_s-meson, as [14]

$$\begin{aligned}
\langle 0|\bar{s}_\alpha(x)h_{v\beta}(0)|B_s(v)\rangle &= -\frac{if_Bm_B}{4}\int_0^\infty d\omega\, e^{-i\omega v.x}\left\{(1+\not{v})\left[\varphi_+(\omega)-\frac{\not{x}}{2v.x}(\varphi_+(\omega)-\varphi_-(\omega))\right]\gamma_5\right\}_{\beta\alpha},\\
\langle 0|\bar{s}_\alpha(x)G_{\lambda\rho}(ux)h_{v\beta}(0)|B_s(v)\rangle &= \frac{f_Bm_B}{4}\int_0^\infty d\omega\int_0^\infty d\xi e^{-i(\omega+u\xi)v.x}\Big\{(1+\not{v})\Big[(v_\lambda\gamma_\rho-v_\rho\gamma_\lambda)\,(\Psi_A(\omega,\xi)-\Psi_V(\omega,\xi))\\
&\quad -i\sigma_{\lambda\rho}\Psi_V(\omega,\xi)-\frac{x_\lambda v_\rho-x_\rho v_\lambda}{v.x}X_A(\omega,\xi)+\frac{x_\lambda\gamma_\rho-x_\rho\gamma_\lambda}{v.x}Y_A(\omega,\xi)\Big]\gamma_5\Big\}_{\beta\alpha},
\end{aligned}\tag{12}$$

where φ_+ and φ_- are the two-particle DA's and Ψ_A, Ψ_V, X_A and Y_A are four independent three-particle DA's of B_s-meson.

To calculate the correlation functions in terms of the two- and three-particle DA's, we substitute Eq. (12) in the matrix elements $\langle 0|\bar{s}_\alpha(x)h_{v\beta}(0)|B_s(v)\rangle$ and $\langle 0|\bar{s}_\alpha(x)G_{\lambda\rho}(ux)h_{v\beta}(0)|B_s(v)\rangle$ that appear in the correlation functions and then the integrals are investigated. Generally, the results of the calculations can be arranged in the following form:

$$\begin{aligned}
\widetilde{\Pi}_\mu^{V-A}(p',\widetilde{q}) &= i\left[\widetilde{\Pi}_+(p',\widetilde{q})\,P_\mu+\widetilde{\Pi}_-(p',\widetilde{q})\,q_\mu\right],\\
\widetilde{\Pi}_\mu^{T}(p',\widetilde{q}) &= \widetilde{\Pi}_T(p',\widetilde{q})\,P_\mu+\ldots,
\end{aligned}\tag{13}$$

and $\widetilde{\Pi}_+$, $\widetilde{\Pi}_-$, and $\widetilde{\Pi}_T$ are presented as follows:

$$\widetilde{\Pi}_j(p',\widetilde{q})=\frac{1}{\pi}\int_0^\infty\frac{d\sigma}{\mathbf{s}(\sigma)-p'^2}\,g_j(\sigma),\tag{14}$$

where $j=+,-,T$. In this representation of the theoretical part of the correlation functions, $\sigma=\omega/m_{B_s}$ is the integration variable, $g_j(\sigma)$ is a function of σ in terms of the B_s-meson DA's, and $\mathbf{s}(\sigma)$ is defined as

$$\mathbf{s}(\sigma)=\sigma\,m_{B_s}^2-\frac{\sigma}{\bar{\sigma}}\,q^2,\tag{15}$$

where $\bar{\sigma}=1-\sigma$.

On the other hand, using the dispersion relation, the theoretical part of the correlation functions $\widetilde{\Pi}_j$ can be related to its imaginary part as

$$\widetilde{\Pi}_j(p',\widetilde{q}) = \frac{1}{\pi}\int_0^\infty ds\,\frac{\mathrm{Im}\widetilde{\Pi}_j(s)}{s-p'^2}.\tag{16}$$

At large spacelike p'^2, the quark-hadron duality approximation is employed as:

$$\frac{1}{\pi}\int_{s_0}^\infty ds\,\frac{\rho_j(s)}{s-p'^2}\simeq\frac{1}{\pi}\int_{s_0}^\infty ds\,\frac{\mathrm{Im}\widetilde{\Pi}_j(s)}{s-p'^2},\tag{17}$$

where $\rho_j(s)$ is the functional part of the tensor ρ_μ^h so that an expression similar to Eq. (13) can be written for it. Using Eqs. (16) and (17) in Eq. (8), and equating the coefficients of the Lorentz structures P_μ and q_μ, leads to the following result.

$$\begin{aligned}
\frac{1}{\pi}\int_0^{s_0} ds\frac{\mathrm{Im}\widetilde{\Pi}_\pm(s)}{s-p'^2} &= \frac{f_{K_0^*}m_{K_0^*}}{m_{K_0^*}^2-p'^2}\,f_\pm(q^2),\\
\frac{1}{\pi}\int_0^{s_0} ds\frac{\mathrm{Im}\widetilde{\Pi}_T(s)}{s-p'^2} &= -\frac{f_{K_0^*}m_{K_0^*}}{m_{B_s}+m_{K_0^*}}\frac{q^2\,f_T(q^2)}{m_{K_0^*}^2-p'^2}.
\end{aligned}\tag{18}$$

Finally, according to Eq. (14) and Eq. (16), it can be concluded that

$$\begin{aligned}
\frac{1}{\pi}\int_0^{\sigma_0}\frac{d\sigma}{\mathbf{s}(\sigma)-p'^2}\,g_\pm(\sigma) &= \frac{f_{K_0^*}m_{K_0^*}}{m_{K_0^*}^2-p'^2}\,f_\pm(q^2),\\
\frac{1}{\pi}\int_0^{\sigma_0}\frac{d\sigma}{\mathbf{s}(\sigma)-p'^2}\,g_T(\sigma) &= -\frac{f_{K_0^*}m_{K_0^*}}{m_{K_0^*}^2-p'^2}\,\frac{q^2\,f_T(q^2)}{m_{B_s}+m_{K_0^*}}.
\end{aligned}\tag{19}$$

To determine the effective threshold σ_0, the continuum threshold of K_0^* meson s_0 is replaced in Eq. (15) instead of $\mathbf{s}$. A quadratic equation is created based on the variable σ. By solving this equation, the value of σ_0 is determined as follows:

$$\sigma_0 = \frac{s_0 + m_{B_s}^2 - q^2 - \sqrt{(s_0 + m_{B_s}^2 - q^2)^2 - 4 s_0 m_{B_s}^2}}{2 m_{B_s}^2}. \tag{20}$$

Applying Borel transformation with respect to the variable p'^2 as:

$$B_{p'^2}(M^2)\left(\frac{1}{p'^2 - m^2}\right)^n = \frac{(-1)^n}{\Gamma(n)} \frac{e^{-\frac{m^2}{M^2}}}{(M^2)^n}, \tag{21}$$

in Eq. (19) in order to suppress the contributions of the higher states, the form factors are obtained via the LCSR in terms of the two- and three-particle DA's of B_s-meson. Our results for $f_+(q^2)$, $f_-(q^2)$, and $f_T(q^2)$ are presented as:

$$\begin{aligned}
f_+(q^2) &= \frac{f_{B_s} m_{B_s}^2}{2 f_{K_0^*} m_{K_0^*}} e^{\frac{m_{K_0^*}^2}{M^2}} \int_0^{\sigma_0} d\sigma\, e^{-\frac{\mathbf{s}(\sigma)}{M^2}} \Bigg\{ \varphi_+(\sigma m_{B_s}) - \frac{\widetilde{\varphi}_+(\sigma m_{B_s}) - \widetilde{\varphi}_-(\sigma m_{B_s})}{\bar{\sigma} m_{B_s}} \\
&+ \int_0^{\sigma m_{B_s}} d\omega \int_{\sigma m_{B_s} - \omega}^{\infty} \frac{d\xi}{\xi} \Bigg\{ \left[(2u+2) \left(\frac{q^2 - \bar{\sigma}^2 m_{B_s}^2}{\bar{\sigma}^3 M^2} + \frac{1}{\bar{\sigma}^2} \right) + \frac{(2u+1) m_{B_s}^2}{\bar{\sigma} M^2} \right] \frac{\Psi_A(\omega,\xi) - \Psi_V(\omega,\xi)}{m_{B_s}^2} \\
&+ \frac{6u}{\bar{\sigma} M^2} \Psi_V(\omega,\xi) + \left[(2u-1) \left(\frac{q^2 - \bar{\sigma}^2 m_{B_s}^2}{\bar{\sigma}^3 M^4} + \frac{1}{\bar{\sigma}^2 M^2} \right) + \frac{3}{\bar{\sigma}^2 M^2} \right] \frac{\widetilde{X}_A(\omega,\xi)}{m_{B_s}} - \frac{4(u+3)}{\bar{\sigma}^2 M^2} \frac{\widetilde{Y}_A(\omega,\xi)}{m_{B_s}} \Bigg\} \Bigg\}, \\
f_-(q^2) &= -\frac{f_{B_s} m_{B_s}^2}{2 f_{K_0^*} m_{K_0^*}} e^{\frac{m_{K_0^*}^2}{M^2}} \int_0^{\sigma_0} d\sigma\, e^{-\frac{\mathbf{s}(\sigma)}{M^2}} \Bigg\{ \frac{(1+\sigma)}{\bar{\sigma}} \varphi_+(\sigma m_{B_s}) + \frac{\widetilde{\varphi}_+(\sigma m_{B_s}) - \widetilde{\varphi}_-(\sigma m_{B_s})}{\bar{\sigma} m_{B_s}} \\
&- \int_0^{\sigma m_{B_s}} d\omega \int_{\sigma m_{B_s} - \omega}^{\infty} \frac{d\xi}{\xi} \Bigg\{ \left[(2u+2) \left(\frac{q^2 - \bar{\sigma}^2 m_{B_s}^2}{\bar{\sigma}^3 M^2} + \frac{1}{\bar{\sigma}^2} \right) - \frac{(2u+1)(1+\sigma) m_{B_s}^2}{\bar{\sigma}^2 M^2} \right] \frac{\Psi_A(\omega,\xi) - \Psi_V(\omega,\xi)}{m_{B_s}^2} \\
&+ \frac{6u(1+\sigma)}{\bar{\sigma}^2 M^2} \Psi_V(\omega,\xi) + \left[\frac{(2u-1)(1+\sigma)}{\bar{\sigma}} \left(\frac{q^2 - \bar{\sigma}^2 m_{B_s}^2}{\bar{\sigma}^3 M^4} + \frac{1}{\bar{\sigma}^2 M^2} \right) + \frac{4(u+\bar{\sigma})}{\bar{\sigma}^3 M^2} \right] \frac{\widetilde{X}_A(\omega,\xi)}{m_{B_s}} \\
&+ \frac{4(u+3)}{\bar{\sigma}^2 M^2} \frac{\widetilde{Y}_A(\omega,\xi)}{m_{B_s}} \Bigg\} \Bigg\}, \\
f_T(q^2) &= \frac{f_{B_s} m_{B_s} (m_{B_s} + m_{K_0^*})}{2 f_{K_0^*} m_{K_0^*}} e^{\frac{m_{K_0^*}^2}{M^2}} \int_0^{\sigma_0} d\sigma\, e^{-\frac{\mathbf{s}(\sigma)}{M^2}} \Bigg\{ \frac{\varphi_+(\sigma m_{B_s})}{\bar{\sigma}} + \int_0^{\sigma m_{B_s}} d\omega \int_{\sigma m_{B_s} - \omega}^{\infty} \frac{d\xi}{\xi} \Bigg\{ \left[\frac{6u}{\bar{\sigma}^2 M^2} \right] \Psi_V(\omega,\xi) \\
&+ \left[\frac{2u+1}{\bar{\sigma}^2 M^2} \right] (\Psi_A(\omega,\xi) - \Psi_V(\omega,\xi)) - \left[\frac{q^2 - \bar{\sigma}^2 m_{B_s}^2}{\bar{\sigma}^4 M^4} + 2 \right] \frac{\widetilde{X}_A}{m_{B_s}} \Bigg\} \Bigg\},
\end{aligned} \tag{22}$$

where:

$$u = \frac{\sigma m_{B_s} - \omega}{\xi}, \qquad \widetilde{\varphi}_\pm(\sigma m_{B_s}) = \int_0^{\sigma m_{B_s}} d\tau \varphi_\pm(\tau), \qquad \widetilde{X}_A(\omega,\xi) = \int_0^{\omega} d\tau X_A(\tau,\xi), \qquad \widetilde{Y}_A(\omega,\xi) = \int_0^{\omega} d\tau Y_A(\tau,\xi).$$

III. NUMERICAL ANALYSIS

In this section, our numerical analysis of the form factors f_+, f_- and f_T is presented for the semileptonic $B_s \to K_0^*$ decays. The values are chosen for masses in GeV as: $m_{B_s} = 5.37$, $m_{K_0^*} = (1.43 \pm 0.05)$, $m_\tau = 1.78$, and $m_\mu = 0.11$ [32]. The leptonic decay constants are taken as: $f_{K_0^*} = (427 \pm 85)\,\text{MeV}$ [33], and $f_{B_s} = (230.3 \pm 1.3)\,\text{MeV}$ [34]. Moreover, the continuum threshold of K_0^* meson, s_0 is equal to $(4.4 \pm 0.4)\text{GeV}^2$ [33]. The values of the parameters λ_E^2 and λ_H^2 of the B_s-meson DA's are chosen as: $\lambda_E^2 = (0.01 \pm 0.01)\,\text{GeV}^2$ and $\lambda_H^2 = (0.15 \pm 0.05)\,\text{GeV}^2$[35].

The two-particle DA's of B_s-meson, $\varphi_+(\omega)$ and $\varphi_-(\omega)$ have the most important contribution in estimation of the form factors f_+, f_-, and f_T. The knowledge of the behavior of $\varphi_+(\omega)$ is still rather limited. However, the evolution effects shows that for sufficiently large values of μ, the DA $\varphi_+(\omega)$ satisfies the condition $\varphi_+(\omega) \sim \omega$ as $\omega \to 0$ and falls off slower than $1/\omega$ for $\omega \to \infty$, which implies that the normalization integral of the φ_+ is ultraviolet divergent.

Without considering the radiative $\mathcal{O}(\alpha_s)$ corrections, the ultraviolet behavior of the φ_+ plays no role at the leading order (LO) [36]. Also, the next-to-leading order (NLO) effects have already been taken into account in more elaborated models of φ_+ based on the HQET sum rules [21]. In this work, we use three phenomenological models for the shape of the DA φ_+ as [28]:

$$\begin{aligned}
&\text{Model I}: \varphi_+(\omega) = \left[(1-a) + \frac{a\,\omega}{2\,\omega_0}\right] \frac{\omega}{\omega_0^2}\, e^{-\omega/\omega_0}, && 0 \le a \le 1 \\
&\text{Model II}: \varphi_+(\omega) = \frac{1}{\Gamma(2+b)} \frac{\omega^{1+b}}{\omega_0^{2+b}}\, e^{-\omega/\omega_0}, && -0.5 < b < 1 \\
&\text{Model III}: \varphi_+(\omega) = \frac{\sqrt{\pi}}{2\,\Gamma(3/2+c)} \frac{\omega}{\omega_0^2}\, e^{-\omega/\omega_0}\, U(c, 3/2-c, \omega/\omega_0), && 0 < c < 0.5
\end{aligned} \tag{23}$$

where $U(\alpha, \beta, z)$ is the confluent hypergeometric function of the second kind. In our calculations, we take the upper limiting values for two parameters a and c, hence $a = 1$, $c = 0.5$. It is remarkable that for $b = 1$, the shape of φ_+ in model-II become the same as that in model-I for $a = 1$, therefore we take $b = 0.5$. The corresponding expression of $\varphi_-(\omega)$ for each model is determined by the equation-of-motion constraint in the absence of contributions from the three-particle DA's as [37]:

$$\varphi_-(\omega) = \int_0^1 \frac{d\tau}{\tau}\, \varphi_+(\omega/\tau). \tag{24}$$

The shape parameter ω_0, that is a parameter of B_s-meson, can be converted to $\lambda_B(\mu = 1\ \text{GeV})$ that is the inverse moment of $\varphi_+(\omega, \mu)$ [36]. Prediction of the λ_B value is varied in different models, for example $\lambda_B = (460 \pm 110)$ MeV calculated using the two-point QCD sum rules [21], $\lambda_B = (460 \pm 160)$ MeV estimated via the LCSR approach [13], $\lambda_B = (350 \pm 150)$ MeV adopted in the QCD factorization approach [38], and $\lambda_B = (360 \pm 110)$ MeV inferred from analyzing the $\bar{B}_u \to \gamma l^- \bar{\nu}$ decay by the LCSR [39]. In addition, a central value $\lambda_B > 238$ MeV has been provided by the BELLE collaboration at 90% credibility level [40]. The values of λ_B discussed here, are valid just for $B^{\pm}$-meson and are applicable for B_s only in the SU(3)_F symmetry limit. Recently, the inverse moment of the B_s-meson distribution amplitude has been predicted from the QCD sum rules (QCDSR) as $\lambda_{B_s} = (438 \pm 150)$ MeV [41]. This value is a reasonable choice for the numerical analysis of the semileptonic $B_s \to K_0^*$ form factors. In this work, we take $\omega_0 = \lambda_{B_s}$ and use the value (438 ± 150) MeV for it. The dependence of the two-particle DA's with respect to ω is shown in Fig. 2 for the three models in Eq. (23).

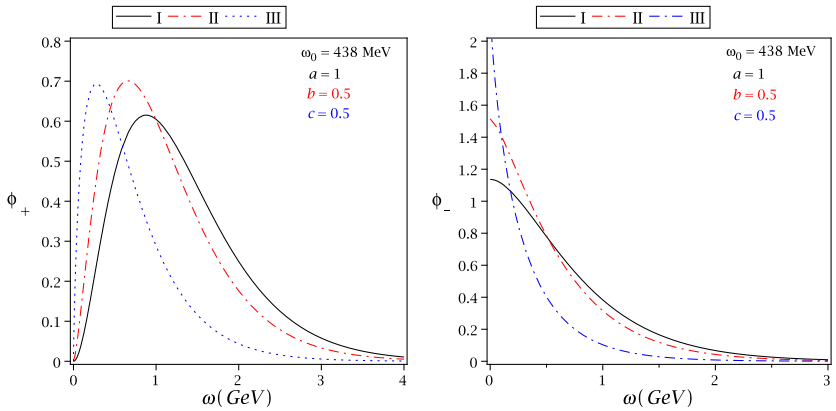


FIG. 2: The dependence of $\varphi_+(\omega)$ and $\varphi_-(\omega)$ on ω for the three models.

Comparing to the two-particle DA's, the contribution of the three-particle DA's is less than 10% in calculations of the form factors. The three-particle DA's are related to a basis of DA's such as ϕ_3, ϕ_4, ψ_4 and ψ_5 with definite twist, as follows [29]:

$$\begin{aligned}
&\Psi_A(\omega,\xi) = \frac{1}{2}\left[\phi_3(\omega,\xi) + \phi_4(\omega,\xi)\right], && \Psi_V(\omega,\xi) = \frac{1}{2}\left[-\phi_3(\omega,\xi) + \phi_4(\omega,\xi)\right], \\
&X_A(\omega,\xi) = \frac{1}{2}\left[-\phi_3(\omega,\xi) - \phi_4(\omega,\xi) + 2\,\psi_4(\omega,\xi)\right], && Y_A(\omega,\xi) = \frac{1}{2}\left[-\phi_3(\omega,\xi) - \phi_4(\omega,\xi) + \psi_4(\omega,\xi) - \psi_5(\omega,\xi)\right].
\end{aligned} \tag{25}$$

So far, several models have been proposed for the shape of ϕ_3, ϕ_4, ψ_4 and ψ_5. Since the structure of φ_+ in three models in Eq. (23) is the exponential form, we choose the exponential model for the functions ϕ_3, ϕ_4, ψ_4 and ψ_5, presented as [29, 30]:

$$\begin{aligned}
\phi_3(\omega,\xi) &= \frac{\lambda_E^2-\lambda_H^2}{6\,\omega_0^5}\,\omega\,\xi^2\,e^{-\frac{\omega+\xi}{\omega_0}}\,, \quad & \phi_4(\omega,\xi) &= \frac{\lambda_E^2+\lambda_H^2}{6\,\omega_0^4}\,\xi^2\,e^{-\frac{\omega+\xi}{\omega_0}}\,,\\
\psi_4(\omega,\xi) &= \frac{\lambda_E^2}{3\,\omega_0^4}\,\omega\,\xi\,e^{-\frac{\omega+\xi}{\omega_0}}\,, & \psi_5(\omega,\xi) &= -\frac{\lambda_E^2}{3\,\omega_0^3}\,\xi\,e^{-\frac{\omega+\xi}{\omega_0}}\,.
\end{aligned} \tag{26}$$

To analyze the form factors f_+, f_-, and f_T, the value of the Borel parameter M^2 must also be determined. The Borel parameter M^2 is not physical quantity, so the physical quantities, form factors, should be independent of it. The working region for M^2 is determined by requiring that the contributions of the higher states and continuum are effectively suppressed. The dependence of the form factors f_+, f_- and f_T on the Borel parameter M^2 is shown in Fig. 3, for the three models in $\omega_0 = 438\,\text{MeV}$, and $q^2 = 0\,\text{GeV}^2$. This figure shows a good stability of the form

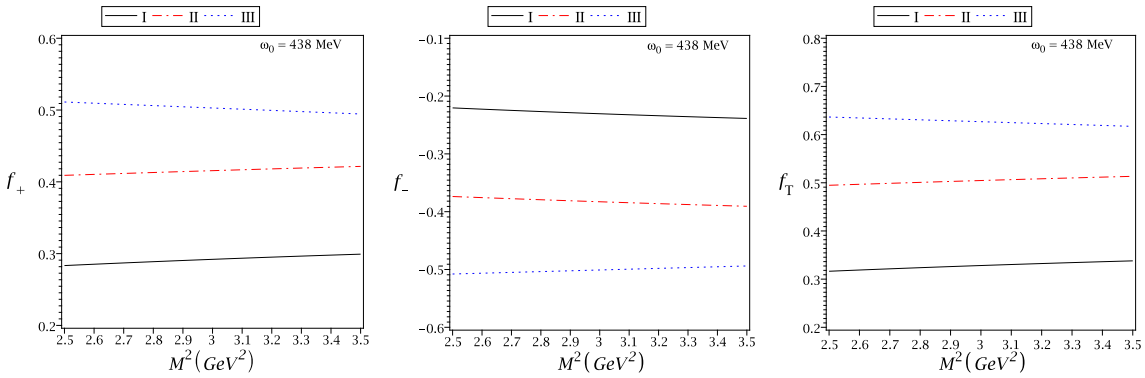


FIG. 3: The dependence of the form factors f_+, f_- and f_T on the Borel parameter M^2 for the three models in $\omega_0 = 438\,\text{MeV}$, and $q^2 = 0\,\text{GeV}^2$.

factors with respect to the Borel parameter in the interval: $2.5\,\text{GeV}^2 \leq M^2 \leq 3.5\,\text{GeV}^2$. We take $M^2 = 3\ \text{GeV}^2$ in our calculations. Uncertainties originated from the Borel parameter M^2 in this region, are about 5%.

Having all these input values and parameters, we proceed to carry out numerical calculations. Inserting the values of the masses, leptonic decay constants, continuum threshold, Borel mass, the parameters of the B_s-meson DA's such as ω_0 and other quantities that appear in the form factors in Eq. (22), we can calculate the form factors of the semileptonic $B_s \to K_0^*$ transitions at zero momentum transfer, $q^2 = 0\,\text{GeV}^2$. Table I shows central values of the form factors for the three models as well as sources of error and also uncertainties caused by them, separately. As can be seen ω_0 and $f_{K_0^*}$ are the most significant sources of theory uncertainties.

Taking into account all the uncertainty values except ω_0, the numerical values of the form factors f_+, f_- and f_T in $q^2 = 0\,\text{GeV}^2$ are presented in Table II for the three models. This table also includes a comparison of our results with the predictions of other approaches such as the LCSR with the light-meson DA's [42–44], perturbative QCD (PQCD) [45] and QCDSR method [46, 47]. As can be seen, there is a very good agreement between our results in model II and predictions of the conventional LCSR with the light-meson DA's in S2 [42]. As a result, our calculations confirm scenario 2 for describing the scalar meson K_0^*.

Due to the presence of cutoff in the QCD calculations, we look for a parametrization of the form factors to extend our results to the full physical region, $0 \leq q^2 \leq (m_{B_s} - m_{K_0^*})^2$. Through fitting the results of the LCSR among the region $0 < q^2 < 8\,\text{GeV}^2$, we extrapolate them with the pole model parametrization

$$f_i(q^2) = \frac{f_i(0)}{1-\alpha(q^2/m_{B_s}^2)+\beta(q^2/m_{B_s}^2)^2}, \tag{27}$$

with the constants α and β determined from the fitting procedure. The values of the parameters α and β are presented in Table III for the three models. The values of parameter $f_i(0)$ expressed the form factor results at $q^2 = 0\,\text{GeV}^2$ were listed in Table II, before.

The dependence of the form factors f_+, f_- and f_T on q^2, for the three models, is shown in Fig. 4. In this work, the form factors are estimated in the LCSR approach up to the three-particle DA's of the B_s-meson. Our calculations show

TABLE I: Central values of the form factors for the three models, as well as sources of error and also uncertainties of the form factors. The uncertainties Δ caused by the variations of the input parameters ($\delta\omega_0 = \pm 0.150$ GeV, $\delta f_{K_0^*} = \pm 0.085$ GeV, $\delta s_0 = \pm 0.4$ GeV^2, $\delta m_{K_0^*} = \pm 0.05$ GeV, $\delta f_{B_s} = \pm 0.001$ GeV, $\delta\lambda_E^2 = \pm 0.01$ GeV^2, $\delta\lambda_H^2 = \pm 0.05$ GeV^2, $\delta M^2 = \pm 0.5$ GeV^2).

Model	Form Factor	Central Value	$\Delta(\omega_0)$	$\Delta(f_{K_0^*})$	$\Delta(s_0)$	$\Delta(m_{K_0^*})$	$\Delta(f_{B_s})$	$\Delta(\lambda_E^2)$	$\Delta(\lambda_H^2)$	$\Delta(M^2)$
I	$f_+(0)$	$+0.283$	$^{+0.252}_{-0.114}$	$^{+0.070}_{-0.047}$	$^{+0.024}_{-0.027}$	$^{+0.004}_{-0.003}$	$^{+0.002}_{-0.003}$	$^{+0.000}_{-0.000}$	$^{+0.004}_{-0.004}$	$^{+0.006}_{-0.007}$
	$f_-(0)$	-0.228	$^{+0.114}_{-0.262}$	$^{+0.038}_{-0.056}$	$^{+0.027}_{-0.024}$	$^{+0.003}_{-0.003}$	$^{+0.002}_{-0.002}$	$^{+0.002}_{-0.002}$	$^{+0.002}_{-0.001}$	$^{+0.011}_{-0.008}$
	$f_T(0)$	$+0.324$	$^{+0.326}_{-0.145}$	$^{+0.080}_{-0.054}$	$^{+0.030}_{-0.034}$	$^{+0.007}_{-0.006}$	$^{+0.003}_{-0.003}$	$^{+0.000}_{-0.001}$	$^{+0.001}_{-0.002}$	$^{+0.009}_{-0.012}$
II	$f_+(0)$	$+0.412$	$^{+0.279}_{-0.145}$	$^{+0.102}_{-0.069}$	$^{+0.025}_{-0.030}$	$^{+0.006}_{-0.005}$	$^{+0.003}_{-0.004}$	$^{+0.000}_{-0.000}$	$^{+0.003}_{-0.004}$	$^{+0.005}_{-0.005}$
	$f_-(0)$	-0.369	$^{+0.149}_{-0.293}$	$^{+0.061}_{-0.092}$	$^{+0.029}_{-0.027}$	$^{+0.004}_{-0.006}$	$^{+0.003}_{-0.004}$	$^{+0.001}_{-0.001}$	$^{+0.001}_{-0.002}$	$^{+0.009}_{-0.009}$
	$f_T(0)$	$+0.495$	$^{+0.363}_{-0.186}$	$^{+0.123}_{-0.082}$	$^{+0.033}_{-0.038}$	$^{+0.011}_{-0.009}$	$^{+0.004}_{-0.004}$	$^{+0.001}_{-0.001}$	$^{+0.002}_{-0.001}$	$^{+0.009}_{-0.009}$
III	$f_+(0)$	$+0.511$	$^{+0.195}_{-0.124}$	$^{+0.127}_{-0.085}$	$^{+0.015}_{-0.018}$	$^{+0.008}_{-0.005}$	$^{+0.005}_{-0.004}$	$^{+0.000}_{-0.000}$	$^{+0.004}_{-0.003}$	$^{+0.013}_{-0.007}$
	$f_-(0)$	-0.506	$^{+0.127}_{-0.188}$	$^{+0.084}_{-0.125}$	$^{+0.019}_{-0.014}$	$^{+0.006}_{-0.007}$	$^{+0.005}_{-0.004}$	$^{+0.001}_{-0.001}$	$^{+0.002}_{-0.001}$	$^{+0.005}_{-0.008}$
	$f_T(0)$	$+0.644$	$^{+0.243}_{-0.158}$	$^{+0.161}_{-0.107}$	$^{+0.019}_{-0.023}$	$^{+0.014}_{-0.011}$	$^{+0.006}_{-0.005}$	$^{+0.001}_{-0.000}$	$^{+0.002}_{-0.001}$	$^{+0.013}_{-0.007}$

TABLE II: The form factors of the semileptonic $B_s \to K_0^*$ transitions at zero momentum transfer from the three models and different approaches.

Method		$f_+(0)$	$f_-(0)$	$f_T(0)$
This work	(I)	$+0.28^{+0.11}_{-0.09}$	$-0.10^{+0.09}_{-0.19}$	$+0.32^{+0.13}_{-0.11}$
	(II)	$+0.41^{+0.14}_{-0.12}$	$-0.37^{+0.11}_{-0.14}$	$+0.50^{+0.18}_{-0.14}$
	(III)	$+0.51^{+0.16}_{-0.12}$	$-0.51^{+0.12}_{-0.16}$	$+0.64^{+0.22}_{-0.15}$
LCSR(S2)	[42]	$+0.42^{+0.13}_{-0.08}$	$-0.34^{+0.10}_{-0.10}$	$+0.52^{+0.18}_{-0.08}$
LCSR(S2)	[43]	$+0.39^{+0.04}_{-0.04}$	$-0.25^{+0.05}_{-0.05}$	$+0.41^{+0.04}_{-0.04}$
LCSR(S2)	[44]	$+0.44$	-0.44	$--$
PQCD(S2)	[45]	$+0.56^{+0.16}_{-0.13}$	$--$	$+0.72^{+0.27}_{-0.17}$
LCSR(S1)	[44]	$+0.10$	-0.10	$--$
PQCD(S1)	[45]	$-0.32^{+0.06}_{-0.07}$	$--$	$-0.41^{+0.08}_{-0.09}$
QCDSR	[46]	$+0.24 \pm 0.10$	$--$	$--$
QCDSR	[47]	$+0.25 \pm 0.05$	-0.17 ± 0.04	$+0.21 \pm 0.04$

that the most contributions comes from the two-particle functions $\varphi_\pm$ for all form factors, so that the contributions of the three-particle DA's are less than 10% of the total. The contributions of the two- and three-particle DA's in the form factors depict in Fig. 5 for model II, separately.

The form factors at large recoil should satisfy the following relations [48]:

$$f_T(q^2) = \frac{m_{B_s} + m_{K_0^*}}{m_{B_s}} f_+(q^2) = -\frac{m_b}{m_{B_s} - m_{K_0^*}} f_-(q^2). \tag{28}$$

Figuer 6 shows that the computed form factors from the LCSR with the B_s-meson DA's for the three models satisfy the relations in Eq. (28), by considering the errors.

TABLE III: The parameters α and β obtained for the form factors of the semileptonic $B \to K_0^*$ transitions for the three models.

Form Factor	$f_+(q^2)$			$f_-(q^2)$			$f_T(q^2)$		
Model	I	II	III	I	II	III	I	II	III
α	-0.14	-0.24	-0.49	$+0.09$	$+0.19$	$+0.46$	-0.14	-0.27	-0.60
β	$+0.26$	$+0.63$	$+3.89$	-0.14	-0.45	-3.76	$+0.25$	$+0.69$	$+5.00$

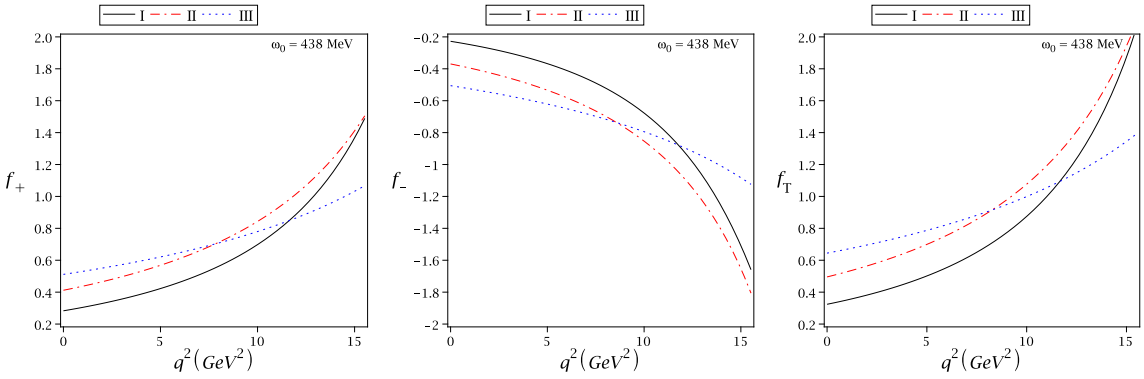


FIG. 4: The dependence of the form factors $f_+(q^2)$, $f_-(q^2)$ and $f_T(q^2)$ of the semileptonic $B_s \to K_0^*$ transitions on q^2 for the three models.

With the derived transition form factors, one can proceed to perform the calculations on some interesting observables in phenomenology, such as decay rate, polarization asymmetry, and forward-backward asymmetry. Note that the forward-backward asymmetry for the decay mode $B_s \to K_0^* l^+ l^-$ is exactly equal to zero in the SM [49].

The effective Hamiltonian for $b \to u l \bar{\nu}_l$ transition is

$$\mathcal{H}_{\rm eff}(b \to u l \bar{\nu}_l) = \frac{G_F}{\sqrt{2}} V_{ub}\, \bar{u}\gamma_\mu(1-\gamma_5) b\; \bar{l}\gamma^\mu(1-\gamma_5)\nu_l\,. \tag{29}$$

With this Hamiltonian, the q^2 dependant decay width $\frac{d\Gamma}{dq^2}$ can be expressed as [44]

$$\frac{d\Gamma}{dq^2}(B_s \to K_0^*\, l\, \bar{\nu}_l) = \frac{G_F^2 |V_{ub}|^2}{384\,\pi^3\, m_{B_s}^3} \frac{(q^2-m_l^2)^2}{(q^2)^3} \sqrt{(m_{B_s}^2 - m_{K_0^*}^2 - q^2)^2 - 4\,q^2\, m_{K_0^*}^2}\; \Big\{(m_l^2 + 2q^2)$$
$$\times \sqrt{(m_{B_s}^2 - m_{K_0^*}^2 - q^2)^2 - 4q^2 m_{K_0^*}^2}\; f_+^2(q^2) + 3\, m_l^2\, (m_{B_s}^2 - m_{K_0^*}^2)^2 \left[f_+(q^2) + \frac{q^2}{m_{B_s}^2 - m_{K_0^*}^2} f_-(q^2)\right]^2\Big\}, \tag{30}$$

where $V_{ub} = (3.82 \pm 0.24) \times 10^{-3}$, and m_l is the mass of the lepton. Integrating Eq. (30) over q^2 in the whole physical region $m_l^2 \le q^2 \le (m_{B_s} - m_{K_0^*})^2$, and using the total mean lifetime $\tau_{B_s} = (1.509 \pm 0.004)\; ps$ [32], we present the branching ratio values of semileptonic decays $B_s \to K_0^*\, l\, \bar{\nu}_l$, $(l = \mu, \tau)$ in Table IV, for the three models. Here, we should also stress that the results obtained for the electron are very close to the results of the muon, and for this reason, we only present the branching ratios for the muon in our table. This table contains the results estimated via the conventional LCSR with the light-meson DA's [42] and PQCD [45] through S2 as well as QCDSR [46] approaches. Considering the range of errors, the values obtained in this work are in a logical agreement with the LCSR and PQCD results. Especially, the obtained values of model II are in a good agreement with the conventional LCSR. As can be seen in this table, uncertainties in the values obtained for the branching ratios of the semileptonic decays $B_s \to K_0^*\, l\, \bar{\nu}_l$ are very large. The main source of errors comes from the form factor $f_+(q^2)$. We show the dependency of the differential branching ratios of $B_s \to K_0^*\, l\, \bar{\nu}_l$, $(l = \mu, \tau)$ decays on q^2 for the three models in Fig. 7.

The semileptonic decays $B_s \to K_0^* l^+ l^- / \nu\bar{\nu}$ are induced by the FCNC (Appendix). Using the parametrization of these transitions in terms of the form factors, the differential decay width in the rest frame of B_s-meson can be written

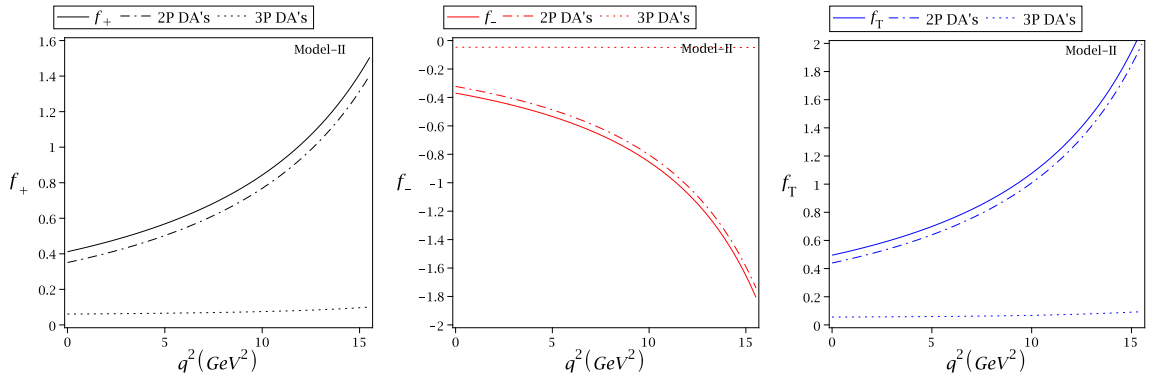


FIG. 5: The contributions of the two-particle DA's (2P DA's) and three-particle DA's (3P DA's) in the form factors $f_+(q^2)$, $f_-(q^2)$ and $f_T(q^2)$ for model II.

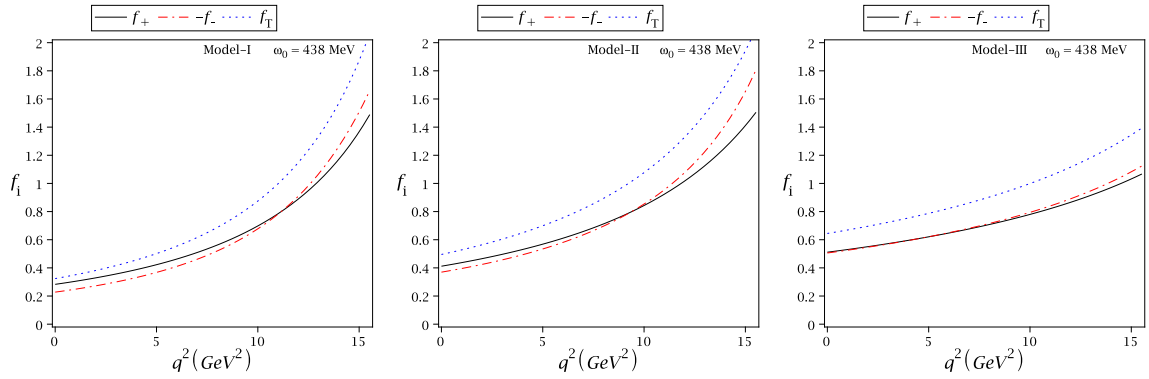


FIG. 6: The dependence of the form factors $f_+(q^2)$, $-f_-(q^2)$ and $f_T(q^2)$ on q^2 via the LCSR with the B_s-meson DA's for the three models.

as:

$$\begin{aligned}
\frac{d\Gamma}{dq^2}(B_s \to K_0^* \nu\bar{\nu}) &= \frac{G_F^2 |V_{td}V_{tb}^*|^2 m_{B_s}^3 \alpha^2}{2^8\pi^5} \frac{|D_\nu(x_t)|^2}{\sin^4\theta_W} \phi^{3/2}(1,\hat{r},\hat{s}) |f_+(q^2)|^2 \,, \\
\frac{d\Gamma}{dq^2}\left(B_s \to K_0^* l^+ l^-\right) &= \frac{G_F^2 |V_{td}V_{tb}^*|^2 m_{B_s}^3 \alpha^2}{3\times 2^9\pi^5} v\, \phi^{1/2}(1,\hat{r},\hat{s}) \left[\left(1+\frac{2\hat{l}}{\hat{s}}\right)\phi(1,\hat{r},\hat{s})\alpha_1 + 12\,\hat{l}\beta_1\right],
\end{aligned} \tag{31}$$

where $\hat{r}$, $\hat{s}$, $\hat{l}$, x_t and $\hat{m}_b$ and the functions v, $\phi(1,\hat{r},\hat{s})$, $D_\nu(x_t)$, α_1 and β_1 are defined as:

$$\begin{aligned}
&\hat{r} = \frac{m_{K_0^*}^2}{m_{B_s}^2}\,, \quad \hat{s} = \frac{q^2}{m_{B_s}^2}\,, \quad \hat{l} = \frac{m_l^2}{m_{B_s}^2}\,, \quad x_t = \frac{m_t^2}{m_W^2}\,, \quad \hat{m}_b = \frac{m_b}{m_{B_s}}\,, \quad v = \sqrt{1-\frac{4\hat{l}}{\hat{s}}}\,, \\
&D_\nu(x_t) = \frac{x_t}{8}\left(\frac{2+x_t}{x_t-1} + \frac{3x_t-6}{(x_t-1)^2}\ln x_t\right), \qquad \phi(1,\hat{r},\hat{s}) = 1+\hat{r}^2+\hat{s}^2-2\hat{r}-2\hat{s}-2\hat{r}\hat{s}\,, \\
&\alpha_1 = \left|C_9^{\rm eff} f_+(q^2) + \frac{2\,\hat{m}_b\, C_7^{\rm eff} f_T(q^2)}{1+\sqrt{\hat{r}}}\right|^2 + |C_{10} f_+(q^2)|^2\,, \\
&\beta_1 = |C_{10}|^2\left[\left(1+\hat{r}-\frac{\hat{s}}{2}\right)|f_+(q^2)|^2 + \left(1-\hat{r}\right)\mathrm{Re}(f_+(q^2)f_-^*(q^2)) + \frac{1}{2}\hat{s}|f_-(q^2)|^2\right].
\end{aligned} \tag{32}$$

These expressions contain the Wilson coefficients $C_7^{\rm eff} = -0.313$, $C_9^{\rm eff}$ (see Appendix) and $C_{10} = -4.669$, the CKM matrix elements $|V_{td}V_{tb}^*| = 0.008$, the form factors related to the fit functions, series of functions and constants.

TABLE IV: The branching ratio values of $B_s \to K_0^* \, l \, \bar{\nu}_l$ for the three models and different approaches.

Mode	This work			LCSR (S2) [42]	PQCD (S2) [45]	QCDSR [46]
	I	II	III			
$\mathrm{Br}(B_s \to K_0^* \mu \, \nu_\mu) \times 10^4$	$0.99^{+0.89}_{-0.37}$	$1.67^{+1.32}_{-0.53}$	$1.90^{+1.48}_{-0.63}$	$1.30^{+1.30}_{-0.40}$	$2.45^{+1.77}_{-1.05}$	$0.36^{+0.38}_{-0.24}$
$\mathrm{Br}(B_s \to K_0^* \tau \, \nu_\tau) \times 10^4$	$0.49^{+0.33}_{-0.17}$	$0.71^{+0.57}_{-0.26}$	$0.65^{+0.55}_{-0.24}$	$0.52^{+0.57}_{-0.18}$	$1.09^{+0.82}_{-0.47}$	$--$

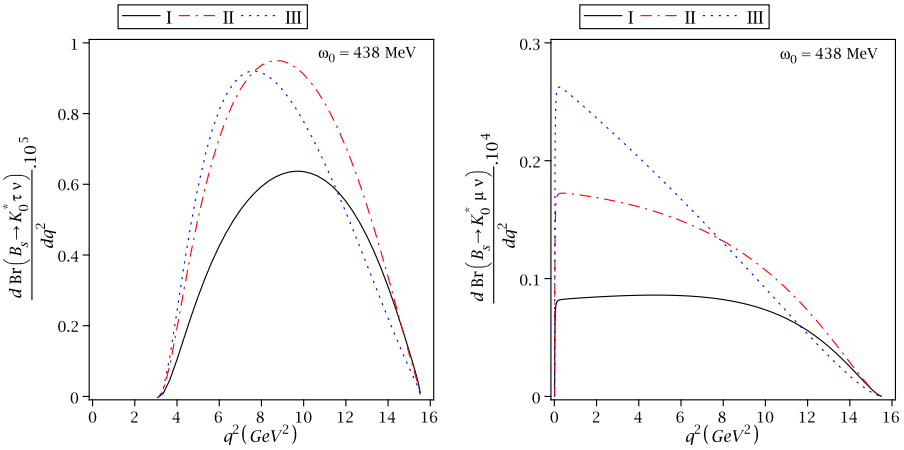


FIG. 7: Differential branching ratios of the semileptonic $B \to K_0^* l \nu_l$ decays on q^2 for the three models.

Integrating Eq. (31) over q^2 in the physical region $4m_l^2 \leq q^2 \leq (m_{B_s} - m_{K_0^*})^2$, and using τ_{B_s}, the branching ratio results of the $B_s \to K_0^* l^+ l^- / \nu\bar{\nu}$ are obtained for the three models as presented in Table V. In this table, we show only the values obtained by considering the short distance (SD) effects contributing to the Wilson coefficient C_9^{eff} for charged lepton case. Predictions by the QCDSR [47], are smaller than those obtained in this work, because of their estimated form factors are smaller than ours (see Table II).

TABLE V: The branching ratios of the semileptonic $B_s \to K_0^* l^+ l^- / \nu\bar{\nu}$ decays for the three models, including only the SD effects.

Mode	This work			QCDSR[47]
	I	II	III	
$\mathrm{Br}(B_s \to K_0^* \nu\bar{\nu}) \quad \times 10^7$	$0.98^{+0.55}_{-0.27}$	$1.66^{+0.95}_{-0.46}$	$1.89^{+1.07}_{-0.52}$	0.25 ± 0.12
$\mathrm{Br}(B_s \to K_0^* \mu^+ \mu^-) \times 10^8$	$1.32^{+0.75}_{-0.36}$	$2.21^{+1.24}_{-0.62}$	$2.48^{+1.38}_{-0.69}$	0.71 ± 0.29
$\mathrm{Br}(B_s \to K_0^* \tau^+ \tau^-) \times 10^9$	$0.61^{+0.34}_{-0.17}$	$0.63^{+0.35}_{-0.17}$	$0.45^{+0.25}_{-0.12}$	0.35 ± 0.16

It should be noted that we have computed the branching ratio values of $B_s \to K_0^* l^+ l^-$ decays in the naive factorization approximation using the factorizable LO quark-loop, i.e., diagrams (a) and (b) in Fig. 8. In this method, contributions of the O_{1-6} operators have the same form factor dependence as C_9 which can be absorbed into an effective Wilson coefficient C_9^{eff}.

For a complete analysis of the branching ratio values of $B_s \to K_0^* l^+ l^-$ decays at the LO, the contributions of the weak annihilation amplitude of diagram (c) must be added to the form factor amplitude related to diagrams (a) and (b) in Fig. 8. Diagram (c) is related to the nonfactorizable effects at the LO. They arise from electromagnetic corrections to the matrix elements of purely hadronic operators in the weak effective Hamiltonian. Since the matrix elements of the semileptonic operators $O_{9,10}$ can be expressed through $B_s \to K_0^*$ form factors, nonfactorizable corrections contribute to the decay amplitude only through the production of a virtual photon, which then decays into the lepton pair [50, 51]. These contributions for $B_s \to K_0^*(1430)$ decays are actually suppressed by small Wilson coefficients

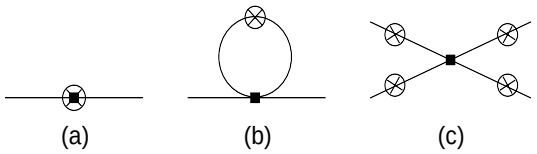


FIG. 8: Factorizable and nonfactorizable contributions in the LO. The circled cross marks the possible insertions of the virtual photon line.

of the penguin operators and can therefore be neglected in the current analysis. In addition to the factorizable and nonfactorizable LO diagrams in Fig. 8, there are factorizable NLO quark-loop and nonfactorizable NLO hard-scattering and soft-gluon contributions in the FCNC $b \to s$ and $b \to d$ transitions and the effects of them must be taken into account [52]. Considering the large current uncertainties due to the form factors, the NLO effects can also be ignored in our calculations.

In this part, the branching ratios including LD effects are presented. In the range of $4m_l^2 \leq q^2 \leq (m_{B_s} - m_{K_0^*})^2$, there are two charm-resonances J/ψ and $\psi(2S)$ used in our calculations. We introduce some cuts around the resonances of J/ψ and $\psi(2S)$ and study the following three regions for muon:

$$\begin{aligned}
&\text{Region-1}: && \sqrt{q^2_{min}} \leq \sqrt{q^2} \leq M_{J/\psi} - 0.20, \\
&\text{Region-2}: && M_{J/\psi} + 0.04 \leq \sqrt{q^2} \leq M_{\psi(2S)} - 0.10, \\
&\text{Region-3}: && M_{\psi(2S)} + 0.02 \leq \sqrt{q^2} \leq m_{B_s} - m_{K_0^*},
\end{aligned} \tag{33}$$

and for tau:

$$\begin{aligned}
&\text{Region-2}: && \sqrt{q^2_{min}} \leq \sqrt{q^2} \leq M_{\psi(2S)} - 0.02, \\
&\text{Region-3}: && M_{\psi(2S)} + 0.02 \leq \sqrt{q^2} \leq m_{B_s} - m_{K_0^*},
\end{aligned} \tag{34}$$

where $\sqrt{q^2_{min}} = 2m_l$. The branching ratio values for muon and tau for the three models with LD effects are listed in Table VI. After numerical analysis, the dependency of the differential branching ratios for $B_s \to K_0^* l^+ l^-/\nu\bar{\nu}$ on q^2

TABLE VI: The branching ratios of the semileptonic $B_s \to K_0^* l^+ l^-$ decays for the three models including LD effects.

Mode	Region-1			Region-2			Region-3			Total		
	I	II	III	I	II	III	I	II	III	I	II	III
$\text{Br}(B_s \to K_0^* \mu^+ \mu^-) \times 10^8$	0.94	1.73	2.14	0.20	0.27	0.21	0.02	0.02	0.01	1.16	2.02	2.36
$\text{Br}(B_s \to K_0^* \tau^+ \tau^-) \times 10^9$	$--$	$--$	$--$	0.21	0.24	0.17	0.31	0.30	0.22	0.52	0.54	0.39

for model II, with and without LD effects is shown in Fig. 9.

Finally, we want to calculate the longitudinal lepton polarization asymmetries for the considered decays. The longitudinal lepton polarization asymmetry formula for $B_s \to K_0^* l^+ l^-$ is given as:

$$P_L = \frac{2v}{(1 + \frac{2\hat{l}}{\hat{s}})\phi(1,\hat{r},\hat{s})\alpha_1 + 12\hat{l}\beta_1} \text{Re}\left[\phi(1,\hat{r},\hat{s})\left(C_9^{eff} f_+(q^2) - \frac{2C_7 f_T(q^2)}{1+\sqrt{\hat{r}}}\right)(C_{10} f_+(q^2))^*\right], \tag{35}$$

where v, $\hat{l}$, $\hat{r}$, $\hat{s}$, $\phi(1,\hat{r},\hat{s}), \alpha_1$ and β_1 were defined before. The dependence of the longitudinal lepton polarization asymmetries for the $B_s \to K_0^* l^+ l^-$, $(l = \mu, \tau)$ decays on the transferred momentum square q^2 for model II, with and without LD effects is plotted in Fig. 10. The averaged values of the lepton polarization asymmetries of these decays for the three models, without the LD contributions are obtained and presented in Table VII. These polarization asymmetries provide valuable information on the flavor changing loop effects in the SM.

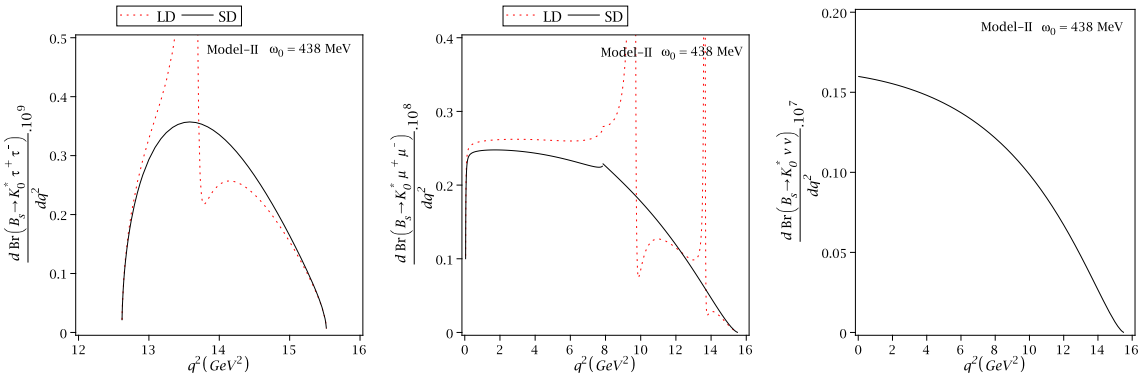


FIG. 9: The differential branching ratios of the semileptonic $B_s \to K_0^* l^+ l^-/\nu\bar{\nu}$ decays ($l = \mu, \tau$) on q^2 for model II. The solid and dotted lines show the results without and with the LD effects, respectively.

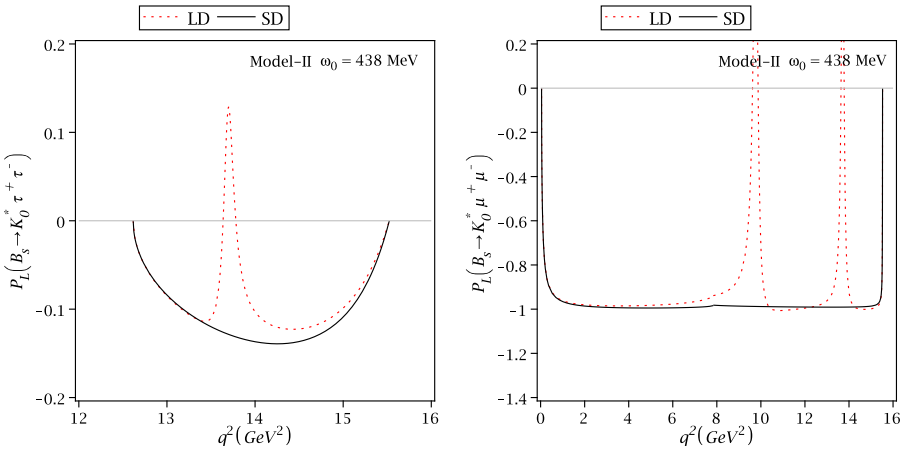


FIG. 10: The dependence of the longitudinal lepton polarization asymmetries on q^2 for model II. The solid and dotted lines show the results without and with the LD effects, respectively.

IV. CONCLUSION

In summary, the transition form factors of the semileptonic $B_s \to K_0$ transitions were calculated via the LCSR with the B_s-meson DA's in the $SU(3)_F$ symmetry limit. We considered the three different models for the shapes of the two-particle DA's, $\varphi_\pm$. It was shown that in estimation of the form factors, the main uncertainties came from the shape parameter ω_0 and the decay constant of the K_0^*-meson. In this work, we used $\omega_0 = \lambda_{B_s}$. Recently, the inverse moment of the B_s-meson distribution amplitude, λ_{B_s} has been predicted from the QCDSR method as $\lambda_{B_s} = (438 \pm 150)$ MeV. There was a very good agreement between our results for the form factors at zero momentum transfer in model II and predictions of the conventional LCSR with the light-meson DA's in scenario 2. Therefore, our calculations confirmed scenario 2 for describing the scalar meson $K_0^*(1430)$. Using the form factors $f_+(q^2)$, $f_-(q^2)$ and $f_T(q^2)$, the branching ratio values for the semileptonic $B_s \to K_0^* l\bar{\nu}_l$ and $B_s \to K_0^* l\bar{l}/\nu\bar{\nu}$ ($l = e, \mu, \tau$) decays were calculated. It is worth mentioning that we computed the branching ratio values of $B_s \to K_0^* l^+ l^-$ decays in the naive factorization approximation. Considering the SD and LD effects, the dependence of the differential branching ratios as well as the longitudinal lepton polarization asymmetries for $B_s \to K_0^* l\bar{l}$ decays were investigated with respect to q^2. Future experimental measurement can give valuable information about these aforesaid decays and the nature of the scalar meson $K_0^*(1430)$.

TABLE VII: Averaged values of the lepton polarization asymmetries of $B_s \to K_0^* l^+ l^-,\ (l = \mu, \tau)$ decays for the three models, without the LD contributions.

Model	I	II	III
$\langle P_L \rangle_\mu$	-0.80	-0.88	-0.98
$\langle P_L \rangle_\tau$	-0.12	-0.13	-0.11

Appendix: The effective weak Hamiltonian of the $b \to d\ l^+l^-$ transition

The effective weak Hamiltonian of the $b \to d\ l^+l^-$ transition has the following form in the SM:

$$\mathcal{H}_{\rm eff}^{b\to d} = -\frac{G_F}{\sqrt{2}}\left(V_{ub}V_{ud}^*\sum_{i=1}^{2}C_i(\mu)O_i^u(\mu) + V_{cb}V_{cd}^*\sum_{i=1}^{2}C_i(\mu)O_i^c(\mu) - V_{tb}V_{td}^*\sum_{i=3}^{10}C_i(\mu)O_i(\mu)\right),$$

where V_{jk} and $C_i(\mu)$ are the CKM matrix elements and Wilson coefficients, respectively. The local operators are current-current operators $O_{1,2}^{u,c}$, QCD penguin operators O_{3-6}, magnetic penguin operators $O_{7,8}$, and semileptonic electroweak penguin operators $O_{9,10}$. The explicit expressions of these operators for $b \to dl^+l^-$ transition are written as [53]

$$\begin{aligned}
&O_1 = (\bar{d}_i c_j)_{V-A}, (\bar{c}_j b_i)_{V-A}, && O_2 = (\bar{d}c)_{V-A}(\bar{c}b)_{V-A},\\
&O_3 = (\bar{d}b)_{V-A}\textstyle\sum_q(\bar{q}q)_{V-A}, && O_4 = (\bar{d}_i b_j)_{V-A}\textstyle\sum_q(\bar{q}_j q_i)_{V-A},\\
&O_5 = (\bar{d}b)_{V-A}\textstyle\sum_q(\bar{q}q)_{V+A}, && O_6 = (\bar{d}_i b_j)_{V-A}\textstyle\sum_q(\bar{q}_j q_i)_{V+A},\\
&O_7 = \frac{e}{8\pi^2}m_b(\bar{d}\sigma^{\mu\nu}(1+\gamma_5)b)F_{\mu\nu}, && O_8 = \frac{g}{8\pi^2}m_b(\bar{d}_i\sigma^{\mu\nu}(1+\gamma_5)T_{ij}b_j)G_{\mu\nu},\\
&O_9 = \frac{e}{8\pi^2}(\bar{d}b)_{V-A}(\bar{l}l)_V, && O_{10} = \frac{e}{8\pi^2}(\bar{d}b)_{V-A}(\bar{l}l)_A,
\end{aligned}$$

where $G_{\mu\nu}$ and $F_{\mu\nu}$ are the gluon and photon field strengths, respectively; T_{ij} are the generators of the $SU(3)$ color group; i and j denote color indices. Labels $(V \pm A)$ stand for $\gamma^\mu(1 \pm \gamma^5)$. The magnetic and electroweak penguin operators O_7, and $O_{9,10}$ are responsible for the SD effects in the FCNC $b \to d$ transition, but the operators O_{1-6} involve both SD and LD contributions in this transition. In the naive factorization approximation, contributions of the O_{1-6} operators have the same form factor dependence as C_9 which can be absorbed into an effective Wilson coefficient $C_9^{\rm eff}$. The effective Wilson coefficient $C_9^{\rm eff}$ includes both the SD and LD effects as

$$C_9^{\rm eff} = C_9 + Y_{SD}(q^2) + Y_{LD}(q^2),$$

where $Y_{SD}(q^2)$ describes the SD contributions from four-quark operators far away from the resonance regions, which can be calculated reliably in perturbative theory as [53, 54]:

$$\begin{aligned}
Y_{SD}(q^2) &= 0.138\,\omega(s) + h(\hat{m}_c, s)C_0 + \lambda_u\, h(\hat{m}_c, s)(3C_1 + C_2) - \frac{1}{2}h(1,s)(4C_3 + 4C_4 + 3C_5 + C_6)\\
&- \frac{1}{2}h(0,s)(2\lambda_u[3C_1 + C_2] + C_3 + 3C_4) + \frac{2}{9}(3C_3 + C_4 + 3C_5 + C_6),
\end{aligned}$$

where $s = q^2/m_b^2$, $\hat{m}_c = m_c/m_b$, $C_0 = 3C_1 + C_2 + 3C_3 + C_4 + 3C_5 + C_6$, $\lambda_u = \frac{V_{ub}V_{ud}^*}{V_{tb}V_{td}^*}$, and

$$\omega(s) = -\frac{2}{9}\pi^2 - \frac{4}{3}{\rm Li}_2(s) - \frac{2}{3}\ln(s)\ln(1-s) - \frac{5+4s}{3(1+2s)}\ln(1-s) - \frac{2s(1+s)(1-2s)}{3(1-s)^2(1+2s)}\ln(s) + \frac{5+9s-6s^2}{3(1-s)(1+2s)},$$

represents the $\mathcal{O}(\alpha_s)$ correction coming from one gluon exchange in the matrix element of the operator O_9 [55], while $h(\hat{m}_c, s)$ and $h(0, s)$ represent one-loop corrections to the four-quark operators O_{1-6} [56]. The functional form of the $h(\hat{m}_c, s)$ and $h(0, s)$ are as:

$$h(\hat{m}_c, s) = -\frac{8}{9}\ln\frac{m_b}{\mu} - \frac{8}{9}\ln\hat{m}_c + \frac{8}{27} + \frac{4}{9}x - \frac{2}{9}(2+x)|1-x|^{1/2}\begin{cases}\left(\ln\left|\frac{\sqrt{1-x}+1}{\sqrt{1-x}-1}\right| - i\pi\right), & \text{for } x \equiv \frac{4\hat{m}_c^2}{s} < 1\\ 2\arctan\frac{1}{\sqrt{x-1}}, & \text{for } x \equiv \frac{4\hat{m}_c^2}{s} > 1\end{cases}$$

and

$$h(0,s) = \frac{8}{27} - \frac{8}{9}\ln\frac{m_b}{\mu} - \frac{4}{9}\ln\ s + \frac{4}{9}i\pi\,.$$

The LD contributions, $Y_{LD}(q^2)$ from four-quark operators near the $u\bar{u}$, $d\bar{d}$ and $c\bar{c}$ resonances cannot be calculated from the first principles of QCD and are usually parametrized in the form of a phenomenological Breit-Wigner formula as [53, 54]:

$$Y_{LD}(q^2) = \frac{3\pi}{\alpha^2}\left\{(C_0 + \lambda_u[3C_1 + C_2])\sum_{V_i = J/\psi,\psi(2S)}\frac{\Gamma(V_i \to l^+l^-)m_{V_i}}{m_{V_i}^2 - q^2 - im_{V_i}\Gamma_{V_i}}\right\}.$$

In the range of $4m_l^2 \leq q^2 \leq (m_{B_s} - m_{K_0^*})^2$, there are two charm-resonances $J/\psi(3.097)$ and $\psi(3.686)$ used in our calculations.

---

[1] J. Weinstein and N. Isgur, Phys. Rev. Lett. **48**, 659 (1982); Phys. Rev. D **27**, 588 (1983); R. Kaminski, L. Lesniak, and J. P. Maillet, Phys. Rev. D **50**, 3145 (1994); G. Janssen, B. C. Pearce, K. Holinde, and J. Speth, Phys. Rev. D **52**, 2690 (1995); R. Kaminski, L. Lesniak, and B. Loiseau, Phys. Lett. B **413**, 130 (1997); J. A. Oller and E. Oset, Nucl. Phys. **A620**, 438 (1997); M. P. Locher, V. E. Markushin, and H. Q. Zheng, Eur. Phys. J. C **4**, 317 (1998).

[2] R. L. Jaffe, Phys. Rev. D **15**, 267 (1977); N. N. Achasov and V.V. Gubin, Phys. Rev. D **56**, 4084 (1997); M. N. Achasov et al., Phys. Lett. B **438**, 441 (1998); D. Black, A. Fariborz, and J. Schechter, Phys. Rev. D **61**, 074001 (2000); R. L. Jaffe and F. Wilczek, Phys. Rev. Lett. **91**, 232003 (2003); L. Maiani, F. Piccinini, A. D. Polosa, and V. Riquer, Phys. Rev. Lett. **93**, 212002 (2004).

[3] H. Y. Cheng, C. K. Chua, and K. C. Yang, Phys. Rev. D **73**, 014017 (2006).

[4] V. M. Belyaev, A. Khodjamirian, and R. Ruckl, Z. Phys. C **60**, 349 (1993).

[5] A. Ali, V. M. Braun, and H. Simma, Z. Phys. C **63**, 437 (1994).

[6] V. M. Belyaev, V. M. Braun, A. Khodjamirian, and R. Ruckl, Phys. Rev. D **51**, 6177 (1995).

[7] A. Khodjamirian, R. Ruckl, S. Weinzierl, and O. I. Yakovlev, Phys. Lett. B **410**, 275 (1997).

[8] P. Ball and V. M. Braun, Phys. Rev. D **58**, 094016 (1998).

[9] E. Bagan, P. Ball, and V. M. Braun, Phys. Lett. B **417**, 154 (1998).

[10] P. Ball, JHEP **9809**, 005 (1998).

[11] P. Ball and R. Zwicky, JHEP **0110**, 019 (2001).

[12] P. Ball and R. Zwicky, Phys. Rev. D **71**, 014015 (2005).

[13] A. Khodjamirian, T. Mannel, and N. Offen, Phys. Lett. B **620**, 52 (2005).

[14] A. Khodjamirian, T. Mannel, and N. Offen, Phys. Rev. D **75**, 054013 (2007).

[15] V. M. Braun and A. Khodjamirian, Phys. Lett. B **718**, 1014 (2013).

[16] V. M. Braun, Y. Ji, and A. N. Manashov, Phys. Rev. D **100**, 014023 (2019).

[17] A. M. Galda and M. Neubert, Phys. Rev. D **102**, 071501 (2020).

[18] W. Wang, Y. M. Wang, J. Xu, and S. Zhao, Phys. Rev. D **102**, 011502 (2020).

[19] S. Zhao and A. V. Radyushkin, Phys. Rev. D **103**, 054022 (2021).

[20] A. G. Grozin and M. Neubert, Phys. Rev. D **55**, 272 (1997).

[21] V. M. Braun, D. Yu. Ivanov, and G. P. Korchemsky, Phys. Rev. D **69**, 034014 (2004).

[22] S. D. Genon and C. T. Sachrajda, Nucl. Phys. **B650**, 356 (2003).

[23] P. Ball and E. Kou, JHEP **0304**, 029 (2003).

[24] S. J. Lee and M. Neubert, Phys. Rev. D **72**, 094028 (2005).

[25] G. Bell, T. Feldmann, Y. M. Wang, and M. W. Y. Yip, JHEP **11**, 191 (2013).

[26] T. Feldmann, B. O. Lange, and Y. M. Wang, Phys. Rev. D **89**, 114001 (2014).

[27] Y. M. Wang and Y. L. Shen, Nucl. Phys. **B898**, 563 (2015).

[28] M. Beneke, V. Braun, Y. Ji, and Y. B. Wei, JHEP **07**, 154 (2018).

[29] V. M. Braun, Y. Ji, and A. N. Manashov, JHEP **1905**, 022(2017).

[30] C. D. Lü, Y. L. Shen, Y. M. Wang, and Y. B. Wei, JHEP **1901**, 024 (2019).

[31] I. I. Balitsky and V. M. Braun, Nucl. Phys. **B311**, 541 (1989).

[32] P. A. Zyla et al. (Particle Data Group), Prog. Theor. Exp. Phys. **2020**, 083C01 (2020).

[33] D. S. Du, J. W. Li, and M. Z. Yang, Phys. Lett. B **619**, 105 (2005).

[34] S. Aoki, Y. Aoki, D. Becirevic et al. (FLAG Review 2019), Eur. Phys. J. C **80**, 113 (2020).

[35] M. Rahimi and M. Wald, Phys. Rev. D **104**, 016027 (2021).

[36] B. O. Lange and M. Neubert, Phys. Rev. Lett. **91**, 102001 (2003).

[37] M. Beneke and T. Feldmann, Nucl. Phys. **B592**, 3 (2001).

[38] M. Beneke, G. Buchalla, M. Neubert, and C. T. Sachrajda, Nucl. Phys. **B591**, 313 (2000).

[39] T. Janowski, B. Pullin, and R. Zwicky, JHEP **12**, 008 (2021).

[40] A. Heller et al. (Belle Collaboration), Phys. Rev. D **91** 112009 (2015).

[41] A. Khodjamirian, R. Mandal, and T. Mannel, JHEP **10**, 043 (2020).

[42] Y. M. Wang, M. J. Aslam, and C. D. Lü, Phys. Rev. D **78**, 014006 (2008).

[43] H. Y. Han, X. G. Wu, H. B. Fu, Q. L. Zhang, and T. Zhong, Eur. Phys. J. C **49**, 78 (2013).

[44] Y. J. Sun, Z. H. Li, and T. Huang, Phys. Rev. D **83**, 025024 (2011).

[45] R. H. Li, C. D. Lü, W. Wang, and X. X. Wang, Phys. Rev. D **79**, 014013 (2009).

[46] M. Z. Yang, Phys. Rev. D **73**, 034027 (2006) [Erratum-ibid. D **73**, 079901 (2006)].

[47] N. Ghahramany and R. Khosravi, Phys. Rev. D **80**, 016009 (2009).

[48] P. Colangelo, F. D. Fazio, and W. Wang, Phys. Rev. D **81**, 074001 (2010).

[49] G. Belanger, C. Q. Geng, and P. Turcotte, Nucl. Phys. **B390**, 253 (1993).

[50] J. Lyon and R. Zwicky, Phys. Rev. D **88**, 094004 (2013).

[51] M. Beneke, Th. Feldmann, and D. Seidel, Eur. Phys. J. C **41**, 173 (2005).

[52] A. Khodjamirian, T. Mannel, A. A. Pivovarov, and Y. M. Wang, JHEP **1009**, 089 (2010); A. Khodjamirian, T. Mannel, and Y. M. Wang, JHEP **02**, 010 (2013); C. Hambrock, A. Khodjamirian, and A. Rusov, Phys. Rev. D **92**, 074020 (2015); A. Khodjamirian and A. V. Rusov, JHEP **08**, 112 (2017).
[53] A. J. Buras and M. Muenz, Phys. Rev. D **52**, 186 (1995).
[54] T. M. Aliev, V. Bashiry, and M. Savci, Phys, Rev, D **72**, 034031 (2005).
[55] M. Jezabek and J. H. Kuhn, Nucl. Phys. **B320**, 20 (1989).
[56] M. Misiak, Nucl. Phys. **B439**, 461 (1995).